HHS Public Access

Author manuscript

Nat Immunol. Author manuscript; available in PMC 2013 June 01.

Published in final edited form as:

Nat Immunol. 2012 December ; 13(12): 1162–1170. doi:10.1038/ni.2446.

Control of RelB during dendritic cell activation integrates canonical and non-canonical NF-κB pathways

Vincent F.-S. Shih[1], **Jeremy Davis-Turak**[1], **Monica Macal**[2], **Jenny Q. Huang**[1], **Julia Ponomarenko**[3], **Jeffrey D. Kearns**[1,4], **Tony Yu**[1], **Riku Fagerlund**[1], **Masataka Asagiri**[1,5], **Elina I. Zuniga**[2], and **Alexander Hoffmann**[1]

[1]Signaling Systems Laboratory, Department of Chemistry and Biochemistry and San Diego Center for Systems Biology (SDCSB)

[2]Division of Biological Sciences

[3]San Diego Supercomputer Center University of California, San Diego 9500 Gilman Dr La Jolla, CA 92093-0375

[5]Center for Innovation in Immunoregulative Technology and Therapeutics, Graduate School of Medicine, Kyoto University, Yoshida-Konoe, Sakyoku, Kyoto 606-8501, Japan

Abstract

The NF-κB protein RelB controls dendritic cell (DC) maturation and may be targeted therapeutically to manipulate T cell responses in disease. Here we report that RelB promoted DC activation not as the expected RelB-p52 effector of the non-canonical NF-κB pathway, but as a RelB-p50 dimer regulated by canonical IκBs, IκBα and IκBε. IκB control of RelB minimized spontaneous maturation but enabled rapid pathogen-responsive maturation. Computational modeling of the NF-κB signaling module identified control points of this unexpected cell-type-specific regulation. Fibroblasts that were engineered accordingly showed DC-like RelB control. Canonical pathway control of RelB regulated pathogen-responsive gene expression programs. This work illustrates the potential utility of systems analyses in guiding the development of combination therapeutics for modulating DC-dependent T cell responses.

Keywords

NF-κB; dendritic cells; computational modeling; systems biology

Correspondence should be addressed to A.H. (ahoffmann@ucsd.edu). Tel. 858 822 4670 Fax 858 822 4671 .

[4]current address: Merrimack Pharmaceuticals, Cambridge, MA

Accession codes The microarray data presented is accessible at GEO, accession number GSE 34990.

Author Contributions V.F-S.S. and A.H. designed the study. V.F-S.S. and M.M. carried out all experimental work with assistance from J.Q.H., T.Y., R.F. and M.A. and guidance from E.I.Z. and A.H. J.D.-T. and J.D.K. carried out the computational modeling work and J.P. the bioinformatic analysis. V.F-S.S. and A.H. wrote the manuscript with contributions from all authors.

Introduction

Dendritic cells (DCs) are specialized sentinel immune cells essential in both innate and adaptive immunity. DC progenitors differentiate to become immature DCs that populate both non-lymphoid and lymphoid tissues and perform immune-surveillance functions. When encountering pathogens or pathogen-associated molecular patterns (PAMPs), immature DCs undergo a maturation program that determines their role in the adaptive immune response[1]. A hallmark of DC maturation is expression of major histocompatibility complex molecules (MHC), T cell costimulatory molecules (CD40, CD80 or CD86) and cytokines (for example, interleukin 23 (IL-23)) in addition to a gene expression program of intracellular factors that enable effective antigen uptake, processing and presentation, and T cell activation. In addition, inflammatory molecules such as nitric oxide and cytokines such as tumor necrosis factor (TNF) and interferon (IFN) underlies DC functions in innate immune responses[2, 3]. DCs have thus attracted attention for engineering or modulating immune-based therapies[4].

The transcription factor NF-κB protein RelB is highly expressed in antigen-presenting cells[5] and critical for DC maturation, their functions as antigen-presenting cells[6] and DC-mediated immunity. Specifically, siRNA-mediated silencing of RelB expression radically altered the DC maturation process and resulted in blunted antigen-specific T cell responses *in vitro* and *in vivo*[7]. RelB-deficient mice revealed deficiencies in splenic DC subsets[8, 9], but other critical roles of RelB in DCs may be masked by other cell types, notably T cells that are misregulated in these null animals. DC-specific deletion of the RelB-controlling kinase NIK resulted in deficient T cell responses[10]. Indeed, the extent of RelB activation determined the tolerance or rejection of allogenic organ transplants by determining the balance of associated activated or regulatory T cells[7]. These insights have prompted investigations of cell-based therapies for autoimmune diseases using RelB-silenced DCs[11].

Despite the potential clinical importance of RelB, the molecular mechanisms that control its activity in DCs have remained unclear. Mouse embryonic fibroblasts (MEFs) have served as a useful model system for many signaling studies. Detailed biochemical studies in MEFs showed that unlike classical NF-κB (the RelA-p50 dimer), RelB is not activated from a latent cytoplasmic pool via the NEMO-dependent, so-called “canonical” signaling pathway, but via the so-called “non-canonical” NF-κB pathway that involves proteolysis and processing of newly synthesized NF-κB2 (p100)[12-14]. Consistent with the critical role of RelB in DCs, non-canonical signaling pathway components such as NIK and *Nf-b2* were reported to be required for proper DC functions[10, 15]. However, RelB was also found to be rapidly activated in DCs by canonical pathway stimuli TNF and lipopolysaccharide (LPS)[16-19] and the canonical signaling pathway component TRAF6 was shown to be essential[9]. These reports suggest that RelB control in DCs may be different than what has been described in MEFs. In DCs, the molecular control mechanisms must provide for constitutive RelB expression to enable rapid and decisive induction of maturation programs following exposure to pathogens or PAMPs, but must limit spontaneous maturation of DCs in their absence.

In this study, we elucidated the molecular mechanisms responsible for regulating RelB in DCs. We used a Systems Biology approach of iterative computational modeling and

quantitative experimental analyses of the NF-κB signaling network in DCs to reveal that RelB activity was limited by classical IκBs, IκBα and IκBε, and regulated via the canonical pathway. Modeling studies identified two DC-specific control points that render RelB subject to regulation by the canonical pathway, and we demonstrated their sufficiency by engineering MEFs accordingly to produce DC-like RelB control. Finally, gene expression profiling revealed that RelB-dependent gene expression programs regulated by the canonical pathway activity control DC-orchestrated immune responses.

Results

Developing a DC-specific model for NFκB signaling

The established view of NF-κB signaling comprises two separate pathways (Fig. 1a)[12]. The canonical pathway, involving the NEMO-dependent kinase IKK, triggers degradation of NF-κB inhibitors, the classical IκBs, IκBα, -β, -ε. Resulting activation of latent RelA- and c-Rel-containing NF-κB dimers controls inflammatory and proliferative gene expression programs. The non-canonical pathway, involving the kinases NIK and IKK1, triggers processing of p100 to p52 and generation of the RelB-p52 transcription factor, which is implicated in cell survival and maturation. To examine NF-κB RelB signaling in DCs in a quantitative manner, we developed a mathematical model that describes the formation and regulation of RelA and RelB dimers in terms of mass action kinetics (Supplementary Notes). The first version of the model involves 41 molecular species, 132 reactions and 53 unique kinetic parameters based on published and newly made measurements that constrain the model to a single parameter set ensemble; it recapitulates well-documented NF-κB control in MEFs[20-22], such as prompt LPS-induced RelA activation and delayed lymphotoxin β-mediated RelB activation (Fig. 1b).

To adapt the model to DCs, we first measured the expression of key NF-κB proteins in bone marrow-derived DCs (BMDCs) in comparison to mouse embryonic fibroblasts (MEFs) and bone marrow-derived macrophages (BMDMs). Relative to the housekeeping gene β-actin (*Actb*), expression of *Rela* mRNA was found to be similar in BMDCs, BMDMs and MEFs, and the relative amount of RelA protein in these cell types correlated (Fig. 1c, top,). In contrast, 3- to 6-fold more *Relb* mRNA and protein expression were observed in BMDCs than MEFs and BMDMs (Fig. 1c, middle, and Supplementary Fig. 1a). p100, encoded by the *Nf-b2* gene, is known to inhibit RelB. We therefore tested if p100 expression correlated with enhanced RelB expression in BMDCs. We did observe 3.5-fold more *Nf-b2* mRNA in BMDCs, but quantitative immunoblotting showed little difference in the p100 protein abundance among the cell types analyzed (Fig. 1c, bottom, and Supplementary Fig. 1b). Lack of correlation between the relative p100 protein and RNA abundance suggested that p100 degradation may be elevated in BMDCs. We noted a 2.5-fold increase of p52 protein in BMDCs, which suggests that both complete p100 degradation and p100 processing to p52 may be occurring in BMDCs (Fig. 1c, bottom, and Supplementary Fig. 1b). Consistent with this hypothesis, protein expression of IKK1, the kinase determining the activity of non-canonical NF-κB pathway, gradually increased during DC differentiation with concomitant p100 processing to p52 (Fig. 1d), potentially via the control of miRNAs[23]. Our data indicate

that DC differentiation involves not only increased expression of RelB, but also elevated constitutive activity of the non-canonical NF-κB signaling pathway.

Based on the measurements, we made specific modifications to the computational model to recapitulate RelB control in DCs (Supplementary Notes). First, we increased *Relb* and *Nf-b2* expression 3-fold, which increased the abundance of RelB but not its nuclear localization. Then we destabilized p100 by the IKK1-dependent pathway to achieve comparable p100 expression as in MEFs (Fig. 1c, bottom right). This change resulted in a substantial increase of nuclear RelB activity (Fig. 1e). To test experimentally if RelB in DCs primarily localizes into the nucleus, we separated BMDCs into cytoplasmic and nuclear extracts but found that more than 75% of the total RelB protein was cytoplasmic (Fig. 1f and Supplementary Fig. 1c,d). Indeed, whereas RelB was more abundant in the cytoplasm of BMDCs than MEFs or BMDMs, p100 was not (Fig. 1g). The fact that the mathematical model, which encodes the known mechanisms of RelB control, failed to reproduce our experimental observations suggested that there may be as yet undescribed regulatory mechanisms that sequester RelB in the cytoplasm.

IκBα restrains RelB:p50 and spontaneous DC maturation

To search for inhibitors of RelB in DCs, we immunoprecipitated RelB from BMDC whole cell lysates and analyzed the associated proteins (Fig. 2a). As expected, p100, the known RelB inhibitor and non-canonical regulator, was found to be associated with RelB. Unexpectedly, IκBα and IκBε, the classical IκB inhibitors regulating the canonical NF-κB pathway, were also immunoprecipitated with RelB, but IκBβ and p105 were not. Interestingly, substantial amounts of p50, known as the binding partner of RelA in the canonical pathway, were found in RelB immunoprecipitates, and this complex was primarily cytoplasmic (Supplementary Fig. 2a,b). Reciprocal immunoprecipitation of various NF-κB inhibitors further confirmed that RelB not only directly interacts with p100 but also associates with IκBα and IκBε in BMDCs (Fig. 2b and Supplementary Fig. 2c), and RelA is associated with IκBα as expected (Supplementary Fig. 2d). Furthermore, the observations that IκB immunoprecipitates did not contain other IκB isoforms confirmed the specificity of the antibodies used and that only one IκB isoform associates with each RelB molecule. Analyses of the amounts of RelB captured (IP) and remaining in the flowthrough (FT) following immunoprecipitation with various IκB antibodies provides a quantitative understanding of RelB protein distribution in BMDCs (Fig. 2c). This analysis revealed that 37% to 45% of RelB was associated with p100 and 12% to 17% with IκBε. Further, we found a substantial proportion of RelB (19% to 34%) associated with IκBα, which prompted us to investigate the function of this interaction further.

To test whether IκBα may inhibit RelB activity in BMDCs, we took advantage of IκBα-deficient mice[22] and developed two strategies to focus our experimental analysis on RelB activity. First, we bred the mice onto a c-Rel-deficient background ($Rel^{-/-}$), then we modified the standard electrophoretic mobility shift assay with κB-site containing probes (κB-EMSA) to include shift-ablating antibodies for RelA, resulting in a specific RelB-EMSA. Using these tools, we found that RelB activity was more than two-fold elevated in IκBα-deficient BMDCs (Fig. 2d). Supershift analysis with antibodies, that were shown to be

specific for p50 and p52 (Supplementary Fig. 2e), revealed that while control BMDCs contained primarily constitutive RelB:p52 activity, ablation of IκBα resulted in a substantial increase in active RelB:p50 dimer, rendering RelB:p50 the predominant NF-κB activity in IκBα-deficient BMDCs (Fig. 2e). We examined the functional consequences of RelB misregulation by monitoring the frequency of matured DCs as indicated by surface expression of the activation markers CD86 and MHC II. Strikingly, IκBα-deficiency resulted in an increased percentage (42% vs. 28%) of $MHCII^{hi}CD86^{hi}$ BMDCs in the absence of external stimuli (Fig. 2f). Although RelB-deficiency does not affect the frequency of $MHCII^{hi}CD86^{hi}$ BMDCs prior to exposure to maturation stimuli (Supplementary Fig. 2f), the inappropriate spontaneous DC maturation phenotype of IκBα-deficient BMDCs was dependent on RelB, as compound deletion of the *Relb* gene fully reversed the phenotype (Fig. 2f). We then examined the antigen-presenting functions of DCs by testing their ability to activate proliferation and cytokine production of antigen-specific T cells in DC–T cell co-cultures (Fig. 2g-i). We found that IκBα-deficiency increased the antigen-presenting functions in BMDC co-cultures with OVA-responsive T cells exposed to ovalbumin peptide, and this effect was largely but not entirely dependent on RelB (Fig. 2h), correlating with the partial RelB-dependence of surface MHC expression (Fig. 2f). However, when these co-cultures were exposed to ovalbumin protein, which must be taken up and processed before being presented, T cell activation showed a near absolute dependence on RelB (Fig. 2i), correlating with previous studies of RelB-deficient DCs[6], and suggesting a specific function for RelB in regulating the antigen uptake and processing program of antigen-presenting cells. Together, these data demonstrate that the classical NF-κB inhibitor, IκBα, not only restrains the expression of RelB by controlling RelA or c-Rel[24], in immature DCs it also has a critical functional role in restraining RelB activity to prevent inappropriate spontaneous maturation.

TLRs activate RelB:p50 via the canonical NFκB pathway

To explore the regulatory consequences of RelB-p50 interactions with IκBα and IκBε proteins during dendritic cell maturation, we incorporated them into the mathematical model as kinetic rate equations, and used the quantitative immunoprecipitation results as constraints in a multi-dimensional parameter optimization protocol (Supplementary Notes). We simulated NF-κB regulation during Toll-like receptor (TLR)-induced dendritic cell maturation using experimentally measured time-course data of the NEMO-dependent IKK kinase activity as an input. Such simulations indicated rapid and substantial activation not only of RelA but also RelB (Fig. 3a). To test this prediction experimentally, BMDCs and MEFs were stimulated with the TLR9 ligand CpG, the TLR2 ligand Pam_3CSK_4 and the TLR4 ligand LPS as well as an agonistic antibody to LTβR to induce the non-canonical NF-κB pathway. To specifically examine the activation profiles of RelA- and RelB-containing NF-κB dimers, we employed the newly developed RelA-EMSA[22] and RelB-EMSA using shift-ablating antibodies for activation domain-containing Rel proteins (Supplementary Fig. 3b). RelA activation was similar in BMDCs and MEFs stimulated with TLR ligands (Fig. 3b, left). Interestingly, we found rapid RelB activation in response to TLR stimuli in BMDCs but not in MEFs, although MEFs do activate RelB at later time points when stimulated with anti-LTβR (Fig. 3b, right, and Supplementary Fig. 3c). Similarly, rapid activation of RelB was observed in splenic DCs stimulated with CpG or Pam_3CSK_4

(Supplementary Fig. 3d). Further, computational simulations suggested that this induced RelB activity consists of RelB-p50 rather than RelB-p52 dimer (Fig. 3c, top). Experimentally, supershift analyses of nuclear extracts revealed that both RelB-p50 and RelB-p52 activities were present in unstimulated conditions, but that CpG stimulation primarily increased RelB-p50 activity (Fig. 3c, bottom, and Supplementary Fig. 3e), unlike LTβR stimulation of MEFs which induces RelB-p52. These data suggest that during DC maturation RelB activation is regulated by the canonical pathway.

A hallmark of canonical signaling is the release of a pre-existing NF-κB dimer, whereas non-canonical signaling involves the stimulus-responsive *de novo* generation of the dimer[12, 25]. In CpG-responding DCs we did not detect increases in protein expression of RelB or p50, or *Relb* mRNA, whereas *Nfkbia* mRNA, encoding IκBα, was induced more than four-fold (Supplementary Fig. 3f). Furthermore, inhibition of protein synthesis by cycloheximide did not block CpG-induced RelB activation whereas resynthesis of IκBα protein was blocked (Supplementary Fig. 3g), suggesting that *de novo* RelB protein synthesis is not required for CpG-inducible RelB activation. In contrast, immunoblotting confirmed that in DCs nuclear accumulation of RelB was accompanied by disappearance of cytoplasmic RelB after CpG stimulation, indicative of stimulus-responsive nuclear translocation of a pre-existing pool of RelB (Supplementary Fig. 3h). Further, inhibition of IKK2 activity, a hallmark of the canonical pathway, by the inhibitor PS-1145 (ref. 26) resulted not only in reduced RelA activity and IκBα protein degradation but also in reduced RelB activation (Supplementary Fig. 3g,i), suggesting that IKK2 signaling is required for RelB activation. We monitored the abundance of known NF-κB inhibitor proteins during the CpG time course: the abundance of the potential RelB inhibitors p100 and p105 remained unaltered; however, IκBα and IκBε were rapidly degraded, correlating with the activation kinetics of RelB activation (Fig. 3d). Importantly, in coimmunoprecipitation assays the amount of IκBα associated with RelB decreased in response to CpG (Fig. 3e). Together, these data suggest that degradation of IκBα allows for the release of RelB from pre-existing IκBα–RelB complexes.

To investigate the role of IκBα in TLR-induced RelB activation, we utilized the mathematical model to computationally simulate the effect of IκB deletions on RelB activation. We found that *in silico* deletion of individual inhibitors had little effect, except in the case of IκBα (Supplementary Fig. 3j). Even compound deficiency of IκBβ, IκBε and IκBδ (which elevated basal RelB activity; Supplementary Fig. 3k), showed robust RelB activation in response to canonical pathway activation, as opposed to greatly diminished activation in an IκBα-deficient model (Fig. 3f). To test these computational modeling predictions, we utilized IκBα-deficient mice[22] and generated *Nfkbib*$^{-/-}$*Nfkbie*$^{-/-}$ *Nfkb2*$^{-/-}$ mice. The lack of protein products was confirmed by immunoblotting (Supplementary Fig. 3l). Indeed, RelB activation was found to be robust in *Nfkbib*$^{-/-}$ *Nfkbie*$^{-/-}$*Nfkb2*$^{-/-}$ BMDCs, whereas IκBα-deficient BMDCs showed a diminished increase and delayed kinetics (Fig. 3g and Supplementary Fig. 3m). Together, these data provide genetic and mechanistic evidence that IκBα is required for CpG-induced RelB activation in DCs.

Engineered MEFs show DC-like RelB control

We previously showed that hallmarks of the NF-κB signaling system in mature but unstimulated DCs are abundant basal RelB expression and basal non-canonical pathway activity. To investigate whether these mechanisms are sufficient and what their relative contributions may be, we performed computational simulations of RelB activation for a range of parameter values governing basal *RelB* mRNA synthesis and NIK protein half-life. These *in silico* analyses showed that activation of RelB mildly increased when either parameter was increased, however, substantial enhancement occurred only when both parameters were concomitantly elevated (Fig. 4a). Our simulations suggest that the DC-specific, rapid RelB activation upon canonical pathway stimulation can be explained by DC-specific, constitutively elevated *RelB* mRNA synthesis and non-canonical IKK activity.

To test this model-derived hypothesis experimentally, we asked whether genetically engineering these two mechanisms into MEFs may be sufficient to allow for DC-like canonical regulation of RelB. We took advantage of MEFs deficient in TRAF3, an E3-ligase controlling NIK degradation[27], to increase constitutive non-canonical signaling. As further suggested by the model simulations, we then transduced a retroviral *Relb* transgene to increase RelB expression about 3-fold relative to untransduced MEFs (Fig. 4b and Supplementary Fig. 4a). Remarkably, the engineered MEFs did indeed show substantial RelB activation in response to LPS (Fig. 4c) or TNF (Supplementary Fig. 4b), whereas the parental control MEFs did not, and RelA activation by these stimuli remained unchanged. Furthermore, neither single genetic alteration produced substantial RelB activation, indicating that enhanced RelB expression and non-canonical pathway activity function synergistically, as predicted by the model, to push RelB into the canonical pathway and render it responsive to TLR agonists. Further, antibody supershift and depletion analysis (Fig. 4d and Supplementary Fig. 4c) confirmed that canonical signaling primarily activated the RelB:p50 dimer (7-fold) rather than the RelB-p52 dimer (2-fold) as observed in DCs and predicted by the computational model (Fig. 3c). Overexpression of a RelB-GFP fusion protein retrovirally transduced into single cells also revealed nuclear translocation upon TNF stimulation in the *Traf3*$^{-/-}$ context but not in control cells (Fig. 4e).

These iterative computational-experimental studies support a model in which the NF-κB protein RelB may function in either non-canonical or canonical pathways (Fig. 4f). When dimerized to p100 or p52, RelB is subject to control by the non-canonical pathway; when dimerized to p50, RelB may be bound by IκBα and IκBε and is regulated by NEMO-dependent canonical signals. Our analysis indicates that low constitutive RelB expression and non-canonical pathway activity characterizes one steady state (found in MEFs) and allows for RelB-p52 activation by stimuli such as LTβ that engage the non-canonical pathway (Supplementary Fig. 4d). High constitutive RelB expression and non-canonical pathway activity characterizes another steady state (found in DCs) and allow for RelB:p50 activation by stimuli such as CpG that engage the canonical pathway (Supplementary Fig. 4e).

RelB and c-Rel cooperate in TLR-induced DC maturation

Given that RelB-p50 is induced by PAMPs during DC maturation, we wondered whether it controls the expression of inflammatory regulators or DC activation markers. Following stimulation with the TLR9 ligand CpG or the TLR2 ligand Pam_3CSK_4 for 24 h, we indeed observed reduced surface expression of DC activation markers MHCII, CD86, CD80 and CD40 in *Relb*$^{-/-}$ DCs (Fig. 5a and Supplementary Fig. 5a,b). Further, we found that expression of pro-inflammatory genes, *Tnf* and *Il23a*, correlated with the kinetics of CpG or Pam_3CSK_4-induced RelB activation and were reduced in *Relb*$^{-/-}$ DCs (Fig. 5b). In EMSAs, activated RelB-p50 was found to be able to bind to DNA probes containing the κB sites found in the *Tnf* and *Il23a* promoters (Fig. 5c), indicating that RelB-p50 can directly interact with these regulatory regions. *In vivo*, recruitment of RelB to the promoter regions of *Tnf* and *Il23a* genes following DC maturation with CpG was also observed using the chromatin immunoprecipitation assay (Fig. 5d).

We noted that RelB bound to consensus κB site sequences[28] associated with the known canonical NF-κB pathway effectors, RelA and c-Rel, rather than the unconventional sequences previously ascribed to RelB in splenic stromal cells[29] or MEFs[20]. Because single knockouts did not show overt defects in $CD11c^+$ cell generation in BM cultures (Supplementary Fig. 5d), we tested whether c-Rel and RelB have overlapping functions in regulating the DC maturation program by examining gene expression in c-Rel and RelB doubly-deficient DCs. Genome-wide expression profiling activated by TLR ligands CpG and Pam_3CSK_4 revealed a group of 157 genes that were statistically significantly down-regulated in *Rel*$^{-/-}$*Relb*$^{-/-}$ BMDCs (Fig. 5e and Supplementary Table 1). To delineate the contribution of RelB in activating these genes, we examined the expression phenotype of the 50 most severely c-Rel–RelB-dependent genes in *Relb*$^{-/-}$ BMDCs stimulated with TLR ligands. Expression phenotypes in fold induction were calculated between wild-type and null DCs, and the order of genes was sorted in increasing degree of RelB-dependency (Fig. 5f and Supplementary Table 2). This analysis revealed a continuous spectrum of RelB-dependency rather than two distinct classes (of RelB-dependent and RelB–independent genes), suggesting an overlap in DNA interaction specificities between c-Rel and RelB dimers. Interestingly, *Tnf* and *Il23a* were identified in this analysis as regulated by both RelB and c-Rel. Quantitative RT-PCR further validated the requirements of RelB and c-Rel in activating *Cxcl2*, *Cd40* and *Il1b* gene expression (Supplementary Fig. 5c).

Given overlapping functions of c-Rel and RelB in regulating DC gene expression programs, we investigated their relationship within the signaling system. Whereas RelA and c-Rel proteins were found to be expressed similarly in wild-type BMDCs and those lacking RelB, *Rel*$^{-/-}$ BMDCs showed decreased RelB protein expression (Fig. 6a). Further, *Relb* transcripts were reduced ~40% in *Rel*$^{-/-}$ BMDC (Fig. 6b). This reduction resulted in severely diminished activation of RelB DNA binding activity in *Rel*$^{-/-}$ BMDCs in response to LPS (Fig. 6c). These data indicate that one of the key determinants of RelB control by the canonical pathway, namely RelB expression, is in fact controlled by c-Rel (Fig. 6d). The feed-forward circuit architecture suggests that expression of RelB in differentiated but immature DCs may reflect the exposure of differentiating cells to c-Rel-inducing stimuli. We therefore tested whether c-Rel-deficient DCs may also be defective in RelB-responsive

gene expression by comparing the expression of RelB-target genes in *Rel*$^{-/-}$ and *Rel*$^{-/-}$*Relb*$^{-/-}$ DCs. Indeed, *Rel*$^{-/-}$ BMDCs showed reductions of surface marker and inflammatory cytokine expression (Supplementary Fig. 6a,b). These data support a model in which RelB acts as a downstream mediator of c-Rel in DC activation programs.

Discussion

The present study revealed how canonical and non-canonical NF-κB signaling pathways integrate to control the RelB transcription factor during DC development and maturation. NF-κB signaling is generally classified as either "canonical" (i.e. NEMO-dependent and involving classical IκBα, -β, and -ε) when activated by acute inflammatory agents or "non-canonical" (i.e. NEMO-independent and involving *Nf-b2*/p100) when activated by developmental signals[12]. NFκB family members were thought to follow this distinction: RelA and c-Rel as effectors of the canonical pathway, and RelB as the effector of the non-canonical pathway, based on its role as a RelB:p52 transcription factor in secondary lymphoid organogenesis. However, we show here that RelB is also an effector of the canonical pathway in DCs.

Specifically, we show that during DC differentiation RelB expression is increased, and that elevated steady-state non-canonical pathway activity results not only in the expected RelB-p52 dimer, but in formation of the RelB-p50 dimer. Unlike RelB-p52, which is mostly nuclear in immature DCs, RelB-p50 is inhibited by the IκB proteins, IκBα and IκBε, which allows for rapid activation of RelB-p50 activity via the canonical pathway upon exposure to maturation stimuli. Conversely, with the recent discovery of IκBδ, [21, 22] chronic inflammatory conditions were found to render RelA an effector of the non-canonical signaling pathway. Thus, both RelA and RelB are potential effectors of the canonical and non-canonical signaling pathways; whether they are functionally relevant effectors is determined by the physiological steady state of the NF-κB signaling system.

Our observations imply that RelB-p50 and RelB-p52 present different molecular surfaces to IκB proteins, providing physiological relevance to previous studies of protein interaction specificities[30, 31]. Similarly, the DNA interaction characteristics of RelB-p50 and RelB-p52 may be distinct[32, 33]. RelB-Arg125 within the RelB-p52 dimer makes an additional base contact with DNA that allows RelB-p52 to recognize a broader range of κB sites. This may account for the RelB-p52 specific function in regulating chemokines involved in secondary lymphoid organeogenesis, such as secondary lymphoid tissue chemokine (SLC), EBI1 ligand chemokine (ELC), B lymphoblastoid cell chemokine (BLC), and stromal cell-derived factor 1α (SDF-1α)[20, 29]. In contrast, RelB-p50 interacts with DNA sequences similarly to RelA-p50 and a role for RelB in TNF production, GM-CSF and Bcl-xl expression has been reported[34, 35]. Together, these studies suggest that the dimerization partner of RelB determines not only the signaling pathway that RelB is responsive to, but also the RelB target gene program.

Why then, would DCs employ RelB as an effector of the canonical NF-κB signaling pathway along with RelA and c-Rel? One possibility is that RelB-p50 target genes are in fact distinct from those controlled by c-Rel or RelA. Our transcriptomic profiling suggests

overlap between c-Rel- and RelB-dependent gene programs, but c-Rel turned out to control RelB expression, thus other tools are required to address the question of RelB-p50 vs. cRel-p50 specificity. A second possibility is that the stimulus-responsive dynamic control of RelB is distinct from RelA or c-Rel. Although RelB-p50 is inhibited by IκBα in resting cells, it may make for a poorer substrate for IκB feedback control than RelA, which is efficiently stripped off the DNA by IκBα [36]. We speculate that the involvement of RelB-p50 in DC biology, ensures irreversible execution of a terminal maturation/activation program in response to transient PAMP exposure.

Mathematical modeling, which is used here to describe biochemical reactions in terms of kinetic rate equations, lends itself as a tool for studying the regulation of signaling networks. Iteratively refined mathematical models of the NF-κB–IκB system have addressed the dynamic and homeostatic control of the NF-κB RelA-p50 dimer by IκB proteins in fibroblasts[21, 22, 37-41]. Within this study, we have developed the first kinetic model that accounts for the generation and regulation of multiple NF-κB dimers, namely RelA- and RelB- containing dimers. Further, we contrasted the steady-state and dynamic control mechanisms in two cell types, MEFs and DCs, and found that the key biochemical differences are two kinetic rate constants (*Relb* mRNA synthesis and NIK halflife); a 3-fold increase was sufficient to shift the *in silico* model from MEF to DC-like regulation of the NF-κB signaling system. This prediction was confirmed experimentally by genetically engineering MEFs to produce DC-like RelB control. Importantly, there was no need to invoke cell-type-specific protein interaction specificities or any other cell-type-specific molecular mechanism. The results indicate that cell-type-specific quantitative control of the steady state of a signaling system may determine seemingly qualitative cell-type-specific properties, such as DC-specific RelB activation by TLRs. As such, kinetic modeling and a quantitative analysis of signaling systems may serve to generate hypotheses not only for mechanistic studies but also for the development of DC-mediated therapeutics.

Methods

Reagents

GM-CSF and IL-4 were from Peprotech. 0.1 μM CpG (Invivogen), 500 ng/ml Pam3CSK4 (Invivogen), 100 ng/ml LPS (Sigma, B5:055) and 0.5 μg/ml LTβR agonist (Biogen, Inc.) were used to stimulate cells. Cycloheximide and IKK2 inhibitor (PS-1145) were from Sigma. Antibodies to RelA (sc-372), RelB (sc-226), c-Rel (sc-70), IκBα (sc-371), IκBβ (sc-945), IκBε (sc-7155), IKK1 (sc-7606), TRAF3 (sc-6933), USF-2 (sc-861), α-tubulin (sc-5286), β-actin (sc-1615) and CD16/CD32 (sc-18867) were from Santa Cruz Biotechnology. p105/p50, p100/p52 and antibody to p100 C-terminus were from National Cancer Institute, Biological Resources Branch, Frederick, MD. NIK antibody (4994) was from Cell Signaling. Immunoprecipitation beads and HRP-conjugated anti-rabbit secondary antibody were from eBioscience.

Animals and Cell Culture

Wild-type and gene-deficient C57BL/6 mice were maintained in accordance with the Animal Care Program at UCSD. *Nfkbia*$^{-/-}$*Tnf*$^{-/-}$ *Rel*$^{-/-}$ and *Nfkbia*$^{-/-}$*Tnf*$^{-/-}$ *Rel*$^{-/-}$*Relb*$^{-/-}$

mice were generated by cross-breeding *Nfkbia*$^{-/-}$*Tnf*$^{-/-}$ with *Rel*$^{-/-}$ and *Relb*$^{-/-}$ mice. *Nfkbib*$^{-/-}$ *Nfkbie*$^{-/-}$*Nfkb2*$^{-/-}$ mice were generated by cross-breeding *Nfkbib*$^{-/-}$, *Nfkbie*$^{-/-}$, and *Nfkb2*$^{-/-}$ mice. *Rel*$^{-/-}$*Relb*$^{-/-}$ mice were generated by cross-breeding *Rel*$^{-/-}$ and *Relb*$^{-/-}$ mice. Primary MEFs were generated from E12.5-14.5 embryos. Bone marrow-derived macrophages (BMDMs) and bone marrow-derived dendritic cells (BMDCs) were made from bone marrow suspensions prepared from mouse femurs. 2×10^6 BM cells seeded on 10 cm plate were cultured for one week with L929-conditioned DMEM medium to derive BMDMs or cultured for 6–11 days with 20 ng/ml GM-CSF and 10 ng/ml IL-4 to derive BMDCs. BMDC medium was replaced on day 3, 6, 8 and floating cells were collected and subjected to experimental analyses as previously described[42]. Typically, day 6-7 BMDCs were used to investigate TLR-induced DC maturation and day 9-11 BMDCs for spontaneous DC maturation studies.

Splenic DC purification

Spleens were cut into small fragments and digested with collagenase D (2 mg/ml, Roche) for 30 min at 37°C followed by incubation with 10 mM EDTA pH 8.0 for 5 min. Single-cell suspension of splenocytes were enriched for CD11c$^+$ cells by immunomagnetic cell sorting using MACS CD11c microbeads (Miltenyi Biotec) according to manufacturer's protocol.

Antibody Staining and Flow Cytometry

Single-cell suspension were collected and blocked with anti-mouse CD16/CD32 in PBS containing 5% FCS for 10 min. Cells were stained with 7-AAD to exclude dead cells and indicated antibodies for DC maturation analyses. All antibodies were purchased from BD Pharmingen: anti-CD11 (HL3), anti-CD40 (3/23), anti-CD80 (16-10A1), anti-CD86 (GL-1), and anti-IA^b (AF6-120.1). Stained cells were acquired in either a FACSCalibur (BD Biosciences) or an Accuri C6 and data analysis was performed with FlowJo software.

Antigen Presentation in DC:T cell co-cultures

GM-CSF derived bone marrow DCs were pulsed with 200 μg whole ovalbumin (Sigma, 5 μM OVA 323-339 (OT-II) peptide (Anaspec, Inc.), or media alone for 2 h at 37 °C. Naive CD4$^+$T cells (5×10^4 cells/well) were obtained by negative enrichment (>90% purity; Stem Cell Technologies) from spleens of B6.Cg-Tg (*TcraTcrb*)425 Cbn/J mice transgenic for ovalbumin 323-339 specific αβTCR (Jackson Laboratory) and labeled with CFSE (Sigma). DCs were washed and cultured with CFSE-labeled CD4$^+$T cells (5×10^4 T cells/well) at the indicated DC:T cell ratios as described[43]. 72 h later, T cells were re-stimulated with 5 μM OT-II peptide for 5 h in the presence of brefeldin A and examined for CFSE dilution and production of TNF, and IL-2 by flow cytometry (BD LSRII). Data were analyzed using FlowJo software (Treestar, Inc.).

Biochemical Analyses

Whole cell extracts were prepared in RIPA buffer and normalized for total protein or cell numbers before immunoblot analysis. Cytoplasmic and nuclear extracts from BMDMs and BMDCs were prepared by high salt extraction buffer (Buffer A: 10 mM HEPES pH 7.9, 10 mM KCl, 0.1 mM EGDA, 0.1 mM EDTA; Buffer C: 20 mM HEPES pH 7.9, 420 mM NaCl,

1.5 mM $MgCl_2$, 0.2 mM EDTA, 25% glycerol). Immunoprecipitation-immunoblotting analysis, electrophoretic mobility shift assay (EMSA), chromatin immunoprecipitation (ChIP) were performed as previously described[21, 44]. In EMSA focusing on RelB-DNA binding activity, nuclear extracts were ablated of RelA and c-Rel-containing DNA binding activities by pre-incubating them with RelA and c-Rel antibodies (Fig. 3b and Supplementary Fig. 3b). Similarly, nuclear extracts were pre-incubated with RelB and c-Rel antibodies when RelA DNA binding activity was the focus (Fig. 3b). Antibody-shift ablation analysis (for RelB, p50 and p52) was performed as previously described[22] and the specificities of antibodies were confirmed (Supplementary Fig. 2e). RNA extraction was performed with RNAeasy Mini Kit (Qiagen) and purified RNA was used for first strand cDNA synthesis with oligo dT and SuperScript RT II (Invitrogen). Quantitative RT-PCR was performed with SYBR Green PCR Master Mix reagent (Stratagene) and Eppendorf Mastercycler realplex system using the Δ(ΔCt) method with β-actin as normalization control and relative to signals in MEFs or respective basal levels to derive fold induction. qRT-PCR and ChIP data shown are representative of three independent experiments (mean ± SD). Quantitation of mRNA and protein abundance are representative of four independent experiments.

Retrovirus-Mediated Gene Transduction

RelB- or RelB-GFP expressing pBabe-puro constructs were generated by standard methods, and co-transfected with pCL.Eco into 293T cells with Lipofectamine™ 2000 transfection reagent (Invitrogen) for 48 h. Supernatant was filtered and used to infect MEFs. Transduced cells were selected with puromycin hydrochloride (Sigma). Images were acquired with a Zeiss Axio Z1 microscope.

Microarray Analysis

RNA was collected from one set of timecourse experiments (1, 8, 24 h) using WT, *Relb*$^{-/-}$, and *Rel*$^{-/-}$*Relb*$^{-/-}$ BMDC stimulated with 0.1 μM CpG (Invivogen) or 500 ng/ml Pam_3CSK_4. Labeling and hybridization to the Illumina v.2 gene expression chip was performed by UCSD Biogem core facility. The raw data was preprocessed and normalized by mloess method[45]. Genes differentially regulated between WT and *Rel*$^{-/-}$ *Relb*$^{-/-}$ BMDCs during TLR stimulation time courses were analyzed by two-class paired SAM (Significant Analysis of Microarray)[46] implemented in the MeV program (Multiple expression Viewer)[47]. Class pairing was defined by corresponding time points between WT and *Rel*$^{-/-}$*Relb*$^{-/-}$ BMDCs. Differentially expressed genes identified at the false discovery rate below 5% were deemed significant. Genes with at least two-fold induction during TLR-elicited DCs maturation are listed in Supplementary Table 1. In heatmaps, expression values of each gene were normalized to its maximum fold induction and clustered by hierarchical clustering with Euclidian distance (Fig. 5e). For phenotyping analyses (Fig. 5f and Supplementary Table 2), the average-fold induction[26] in $\log_2$ scale across either timecourse (CpG and Pam_3CSK_4) was calculated for different genotypes, e.g. FI_{WT}, $FI_{Rel-/-}$, and $FI_{Rel-/-Relb-/-}$. The RelB phenotype was defined as FI_{WT}-$FI_{Rel-/-}$, the c-Rel-RelB phenotype was defined as FI_{WT}- $FI_{Rel-/-Relb-/-}$.

Computational modeling

The RelA–RelB mathematical model (Version 5.0) involving mass action kinetic equations was developed based on a previously published model (Version 3.1)[22] and experimental data[20] that allowed for constraints-based parameterization. Refinement of the model (Version 5.1) and MEF- and DC-specific parameterization were based on experimental data presented in this paper. Computational simulations were performed in Matlab using the ode15s solver. Detailed descriptions are included in Supplemental Notes and biochemical reactions are listed in Supplementary Tables 3, 4.

Statistics

Statistical significance was calculated by two-tailed Student's *t* test with Prism software (GraphPad). Error bars were shown as either s.d. or s.e.m. as indicated.

Supplementary Material

Refer to Web version on PubMed Central for supplementary material.

Acknowledgements

We thank Z. Tao and G. Ghosh for plasmids and recombinant proteins, S. Basak, A. Wu, P. Loriaux, R. Tsui for computational modeling advice, and C. Brown and M. Karin for *Traf3*$^{-/-}$ embryos. This study was supported by GM085763 (AH), GM071573 (AH), AI090935 (AH), GM085325 (JP) and AI081923 (EIZ).

References

1. Banchereau J, Steinman RM. Dendritic cells and the control of immunity. Nature. 1998; 392:245–252. [PubMed: 9521319]
2. Liu YJ. IPC: professional type 1 interferon-producing cells and plasmacytoid dendritic cell precursors. Annu Rev Immunol. 2005; 23:275–306. [PubMed: 15771572]
3. Serbina NV, Salazar-Mather TP, Biron CA, Kuziel WA, Pamer EG. TNF/iNOS-producing dendritic cells mediate innate immune defense against bacterial infection. Immunity. 2003; 19:59–70. [PubMed: 12871639]
4. Steinman RM, Banchereau J. Taking dendritic cells into medicine. Nature. 2007; 449:419–426. [PubMed: 17898760]
5. Carrasco D, Ryseck RP, Bravo R. Expression of relB transcripts during lymphoid organ development: specific expression in dendritic antigen-presenting cells. Development. 1993; 118:1221–1231. [PubMed: 8269849]
6. Zanetti M, Castiglioni P, Schoenberger S, Gerloni M. The role of relB in regulating the adaptive immune response. Annals of the New York Academy of Sciences. 2003; 987:249–257. [PubMed: 12727647]
7. Li M, et al. Immune modulation and tolerance induction by RelB-silenced dendritic cells through RNA interference. J Immunol. 2007; 178:5480–5487. [PubMed: 17442929]
8. Wu L, et al. RelB is essential for the development of myeloid-related CD8alpha-dendritic cells but not of lymphoid-related CD8alpha+ dendritic cells. Immunity. 1998; 9:839–847. [PubMed: 9881974]
9. Kobayashi T, et al. TRAF6 is a critical factor for dendritic cell maturation and development. Immunity. 2003; 19:353–363. [PubMed: 14499111]
10. Hofmann J, Mair F, Greter M, Schmidt-Supprian M, Becher B. NIK signaling in dendritic cells but not in T cells is required for the development of effector T cells and cell-mediated immune responses. The Journal of experimental medicine. 2011; 208:1917–1929. [PubMed: 21807870]

11. Yang H, et al. Suppression of ongoing experimental autoimmune myasthenia gravis by transfer of RelB-silenced bone marrow dentritic cells is associated with a change from a T helper Th17/Th1 to a Th2 and FoxP3+ regulatory T-cell profile. Inflamm Res. 2010; 59:197–205. [PubMed: 19768385]
12. Pomerantz JL, Baltimore D. Two pathways to NF-kappaB. Mol Cell. 2002; 10:693–695. [PubMed: 12419209]
13. Oeckinghaus A, Hayden MS, Ghosh S. Crosstalk in NF-kappaB signaling pathways. Nature immunology. 2011; 12:695–708. [PubMed: 21772278]
14. Derudder E, et al. RelB/p50 dimers are differentially regulated by tumor necrosis factor-alpha and lymphotoxin-beta receptor activation: critical roles for p100. J Biol Chem. 2003; 278:23278–23284. [PubMed: 12709443]
15. Lind EF, et al. Dendritic cells require the NF-kappaB2 pathway for cross-presentation of soluble antigens. J Immunol. 2008; 181:354–363. [PubMed: 18566401]
16. O'Sullivan BJ, Thomas R. CD40 ligation conditions dendritic cell antigen-presenting function through sustained activation of NF-kappaB. J Immunol. 2002; 168:5491–5498. [PubMed: 12023343]
17. Saccani S, Pantano S, Natoli G. Modulation of NF-kappaB activity by exchange of dimers. Mol Cell. 2003; 11:1563–1574. [PubMed: 12820969]
18. Ammon C, Mondal K, Andreesen R, Krause SW. Differential expression of the transcription factor NF-kappaB during human mononuclear phagocyte differentiation to macrophages and dendritic cells. Biochem Biophys Res Commun. 2000; 268:99–105. [PubMed: 10652220]
19. Gasparini C, Foxwell BM, Feldmann M. RelB/p50 regulates CCL19 production, but fails to promote human DC maturation. Eur J Immunol. 2009; 39:2215–2223. [PubMed: 19655301]
20. Basak S, Shih VF, Hoffmann A. Generation and activation of multiple dimeric transcription factors within the NF-kappaB signaling system. Mol Cell Biol. 2008; 28:3139–3150. [PubMed: 18299388]
21. Basak S, et al. A fourth IkappaB protein within the NF-kappaB signaling module. Cell. 2007; 128:369–381. [PubMed: 17254973]
22. Shih VF, et al. Kinetic control of negative feedback regulators of NF-kappaB/RelA determines their pathogen- and cytokine-receptor signaling specificity. Proc Natl Acad Sci U S A. 2009; 106:9619–9624. [PubMed: 19487661]
23. Li T, et al. MicroRNAs modulate the noncanonical transcription factor NF-kappaB pathway by regulating expression of the kinase IKKalpha during macrophage differentiation. Nature immunology. 2010; 11:799–805. [PubMed: 20711193]
24. Wuerzberger-Davis SM, et al. Nuclear export of the NF-kappaB inhibitor IkappaBalpha is required for proper B cell and secondary lymphoid tissue formation. Immunity. 2011; 34:188–200. [PubMed: 21333553]
25. Shih VF, Tsui R, Caldwell A, Hoffmann A. A single NFkappaB system for both canonical and non-canonical signaling. Cell Res. 2011; 21:86–102. [PubMed: 21102550]
26. Waterfield M, Jin W, Reiley W, Zhang M, Sun SC. IkappaB kinase is an essential component of the Tpl2 signaling pathway. Mol Cell Biol. 2004; 24:6040–6048. [PubMed: 15199157]
27. He JQ, et al. Rescue of TRAF3-null mice by p100 NF-kappa B deficiency. The Journal of experimental medicine. 2006; 203:2413–2418. [PubMed: 17015635]
28. Hoffmann A, Natoli G, Ghosh G. Transcriptional regulation via the NF-kappaB signaling module. Oncogene. 2006; 25:6706–6716. [PubMed: 17072323]
29. Bonizzi G, et al. Activation of IKKalpha target genes depends on recognition of specific kappaB binding sites by RelB:p52 dimers. Embo J. 2004; 23:4202–4210. [PubMed: 15470505]
30. Lernbecher T, Kistler B, Wirth T. Two distinct mechanisms contribute to the constitutive activation of RelB in lymphoid cells. Embo J. 1994; 13:4060–4069. [PubMed: 8076601]
31. Dobrzanski P, Ryseck RP, Bravo R. Differential interactions of Rel-NF-kappa B complexes with I kappa B alpha determine pools of constitutive and inducible NF-kappa B activity. Embo J. 1994; 13:4608–4616. [PubMed: 7925301]
32. Fusco AJ, et al. NF-kappaB p52:RelB heterodimer recognizes two classes of kappaB sites with two distinct modes. EMBO Rep. 2009; 10:152–159. [PubMed: 19098713]

33. Moorthy AK, Huang DB, Wang VY, Vu D, Ghosh G. X-ray structure of a NF-kappaB p50/RelB/DNA complex reveals assembly of multiple dimers on tandem kappaB sites. J Mol Biol. 2007; 373:723–734. [PubMed: 17869269]
34. Weih F, Warr G, Yang H, Bravo R. Multifocal defects in immune responses in RelB-deficient mice. J Immunol. 1997; 158:5211–5218. [PubMed: 9164938]
35. Sasaki CY, Ghosh P, Longo DL. Recruitment of RelB to the Csf2 promoter enhances RelA-mediated transcription of granulocyte-macrophage colony-stimulating factor. J Biol Chem. 2011; 286:1093–1102. [PubMed: 21071440]
36. Bergqvist S, et al. Kinetic enhancement of NF-kappaB×DNA dissociation by IkappaBalpha. Proc Natl Acad Sci U S A. 2009; 106:19328–19333. [PubMed: 19887633]
37. Werner SL, Barken D, Hoffmann A. Stimulus specificity of gene expression programs determined by temporal control of IKK activity. Science. 2005; 309:1857–1861. [PubMed: 16166517]
38. O'Dea EL, Kearns JD, Hoffmann A. UV as an amplifier rather than inducer of NF-kappaB activity. Mol Cell. 2008; 30:632–641. [PubMed: 18538661]
39. O'Dea EL, et al. A homeostatic model of IkappaB metabolism to control constitutive NF-kappaB activity. Mol Syst Biol. 2007; 3:111. [PubMed: 17486138]
40. Kearns JD, Basak S, Werner SL, Huang CS, Hoffmann A. IkappaBepsilon provides negative feedback to control NF-kappaB oscillations, signaling dynamics, and inflammatory gene expression. J Cell Biol. 2006; 173:659–664. [PubMed: 16735576]
41. Hoffmann A, Levchenko A, Scott ML, Baltimore D. The IkappaB-NF-kappaB signaling module: temporal control and selective gene activation. Science. 2002; 298:1241–1245. [PubMed: 12424381]
42. Lutz MB, et al. An advanced culture method for generating large quantities of highly pure dendritic cells from mouse bone marrow. J Immunol Methods. 1999; 223:77–92. [PubMed: 10037236]
43. Boonstra A, et al. Flexibility of mouse classical and plasmacytoid-derived dendritic cells in directing T helper type 1 and 2 cell development: dependency on antigen dose and differential toll-like receptor ligation. The Journal of experimental medicine. 2003; 197:101–109. [PubMed: 12515817]
44. Cheng CS, et al. The specificity of innate immune responses is enforced by repression of interferon response elements by NF-kappaB p50. Sci Signal. 2011; 4:ra11. [PubMed: 21343618]
45. Sasik R, Woelk CH, Corbeil J. Microarray truths and consequences. J Mol Endocrinol. 2004; 33:1–9. [PubMed: 15291738]
46. Tusher VG, Tibshirani R, Chu G. Significance analysis of microarrays applied to the ionizing radiation response. Proc Natl Acad Sci U S A. 2001; 98:5116–5121. [PubMed: 11309499]
47. Saeed AI, et al. TM4 microarray software suite. Methods Enzymol. 2006; 411:134–193. [PubMed: 16939790]
48. Giorgetti L, et al. Noncooperative interactions between transcription factors and clustered DNA binding sites enable graded transcriptional responses to environmental inputs. Mol Cell. 2010; 37:418–428. [PubMed: 20159560]

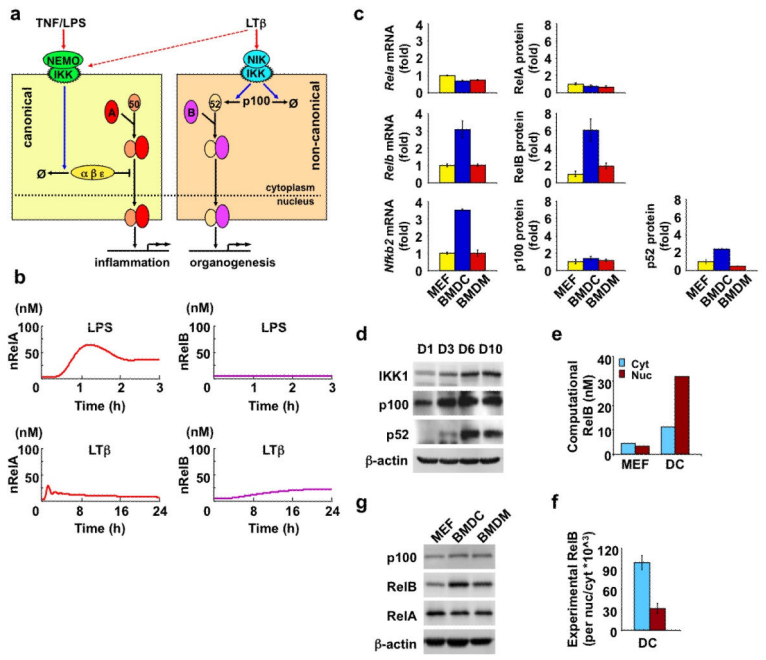

Figure 1. A MEF-based kinetic model does not account for RelB regulation in DCs

(a) Schematic of the distinct canonical and non-canonical NF-κB pathways identified in MEFs[12]. Inflammatory signals lead to activation of the NEMO-containing kinase complex that triggers IκBα, -β, -ε degradation and the release of RelA-p50 into the nucleus. Developmental signals activate NIK–IKK1 kinase complex that results in p100 processing which allows for RelB-p52 nuclear translocation. (The IκBδ pathway is not shown for sake of clarity[21]).

(b) Computational simulations using the MEF-based kinetic model version 5.0-MEF (see Supplementary Notes for details). The timecourse for nuclear RelA or RelB activity induced by LPS or LTβ stimulation are shown.

(c) Quantitation of *Rela*, *Relb* and *Nf-b2* transcript (left, by qRT-PCR) and of RelA, RelB, p100 and p52 protein (right, by immunoblot) numbers per cell in resting MEFs, BMDMs and BMDCs, graphed relative to the respective value in MEFs.

(d) IKK1 and p52 abundance increase during DC differentiation. Whole cell extracts prepared from BMDC cell culture during a differentiation time course were subjected to IKK1 and p100/p52 immunoblotting.

(e) *in silico* simulation of RelB cellular distribution using the mathematical model version 5.0-MEF describing NF-κB activation in MEFs as in Figure 1b or in model version 5.0-DC incorporating DC specific parameters derived from Figure 1c and 1d (see Supplementary Notes for details).

(f) Bar graph showing quantitation of RelB molecules per WT BMDC distributed in cytoplasmic (CE) and nuclear (NE) fraction. Quantitation methods are described in Supplementary Fig. 1.

(g) RelB, RelA and p100 immunoblots of cytoplasmic extracts prepared from the indicated cell types.

Data shown are representative of at least three independent experiments (error bars, s.d.).

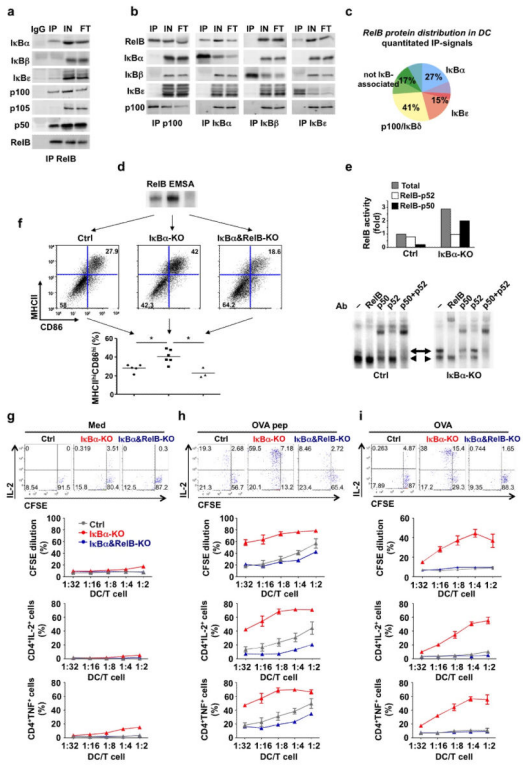

Figure 2. IκBα binding RelB-p50 limits spontaneous DC maturation

(a) RelB interacts with canonical IκBα and IκBε. RelB immunoprecipitates from whole DC extracts were probed for indicated interaction partners by immunoblotting. Fraction of proteins bound to RelB (IP) was compared to whole cell lysates (IN) and flow-through (FT). IgG immunoprecipitates served as an antibody specificity control.

(b) IκBα and IκBε interact with RelB. IκB proteins were probed for their interaction with RelB using co-immunoprecipitation. Immunoblotting with other IκB family members served as negative controls.

(c) NF-κB RelB DNA binding activities revealed by EMSA with nuclear extracts collected from *Rel*$^{-/-}$*Tnf*$^{-/-}$, *Nfkbia*$^{-/-}$*Tnf*$^{-/-}$ *Rel*$^{-/-}$, and *Nfkbia*$^{-/-}$*Tnf*$^{-/-}$ *Rel*$^{-/-}$ *Relb*$^{-/-}$ BMDCs.

(d) Quantitation of total RelB activity, RelB-p50 and RelB-p52 in immature BMDCs from indicated genotypes as revealed by EMSA. Band intensities of the antibody-ablation analysis (bottom) were summed and normalized to the total (panel c) and graphed relative to total RelB activity in WT BMDCs.

(e) Constitutive expression of maturation markers is controlled by RelB. Fractions of CD11c^{+} BMDCs determined by FACS to be MHCII^{hi}CD86^{hi} and MHCII^{lo}CD86^{lo} in indicated genotypes. Dot plots indicate the frequency of MHCII^{hi}CD86^{hi} dendritic cells derived from GM-CSF-cultured *Rel*$^{-/-}$*Tnf*$^{-/-}$ (n=5), *Nfkbia*$^{-/-}$*Tnf*$^{-/-}$ *Rel*$^{-/-}$ (n=6), and *Nfkbia*$^{-/-}$*Tnf*$^{-/-}$ *Rel*$^{-/-}$ *Relb*$^{-/-}$ (n=3) bone marrow cells in individual experiments. *P**<0.01

(f-h) T-cell proliferation in DC:T cell co-cultures using *Tnf*$^{-/-}$, *Nfkbia*$^{-/-}$*Tnf*$^{-/-}$, and *Nfkbia*$^{-/-}$ *Tnf*$^{-/-}$*Relb*$^{-/-}$ BMDCs exposed to medium (f), OVA peptide (g) or OVA protein (h). Top, raw FACS data of CFSE-labeled T-cells stained for IL-2, showing proliferation-associated dye-dilution and IL-2 production. Middle, fraction of divided cells and, bottom,

fraction of T-cells positive for the indicated activation-associated cytokine, graphed as a function of the DC:T cell ratio.

Data shown in (a) (b) (c) (e) are representative of at least three independent experiments. Data in (f-h) are the average of duplicate leukocyte reactions produced for each of two independent BMDC cultures.

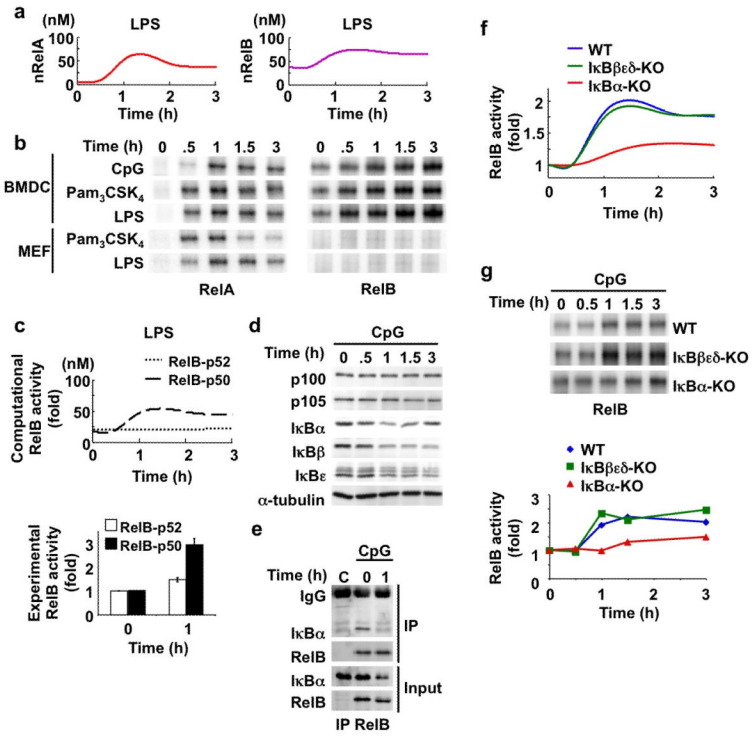

Figure 3. RelB-p50 is rapidly activated during TLR-mediated DC maturation

(a) Computational simulations of LPS-induced RelA and RelB activity during a 3 hour time course using the refined mathematical model version 5.1-DC.

(b) NF-κB RelA (left) and NF-κB RelB (right) DNA binding activities monitored by EMSA. Nuclear extracts from WT BMDCs or WT MEFs activated by indicated stimuli were collected and subjected to EMSA. Equal amounts of nuclear proteins from BMDCs or MEFs were loaded and exposure of images was adjusted to reveal similar RelA peak activity in BMDCs and MEFs.

(c) Computational simulations of RelB-p50 and RelB-p52 activities upon LPS stimulation that sum up to total nuclear RelB activity shown in panel A (top). Quantitation of RelB-p50 and RelB-p52 activities prior and after CpG stimulation were graphed relative to their respective basal activity (bottom).

(d) IκB protein expression profiles induced by CpG. Whole cell extracts prepared from WT BMDCs were subjected to immunoblotting against antibodies as indicated.

(e) Association of IκBα to RelB was monitored during a CpG time course by examining RelB immunoprecipitates from CpG-stimulated WT BMDCs. Immunoprecipitation with *Relb*$^{-/-}$ extracts (C) serves as a control, indicating specificity of RelB antibody.

(f) Computational simulations of CpG-induced RelB activation in mathematical models, based on version 5.1-DC that were deficient in the indicated proteins.

(g) CpG-induced NF-κB RelB DNA binding activities in indicated gene-deficient BMDCs were monitored by EMSA (top). Signals were quantitated and graphed relative to respective resting cells (bottom).

Data shown in (b) (d) (e) (g) are representative of at least three independent experiments. Data shown in (c) is representative of two independent experiments (error bars: s.d.)

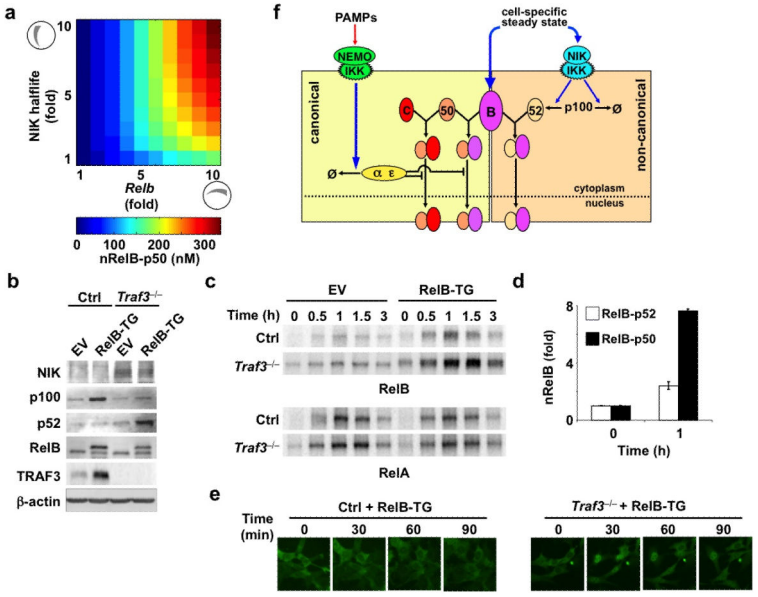

Figure 4. Determinants of RelB's responsiveness to canonical signals

(a) Heatmap depicting how LPS-inducibility of RelB is a function RelB synthesis and NIK halflife. The results derived from *in silico* simulations of peak nuclear RelB-p50 DNA abundance (nM) during an LPS time course when modulating the halflife of NIK (y-axis) and the mRNA synthesis rate of RelB (x-axis).

(b) Immunoblots with indicated antibodies of whole cell extracts collected from control or *Traf3*$^{-/-}$ MEFs reconstituted with empty vector (EV) or RelB transgene (RelB-TG). The top band in the RelB blot represents exogenous protein whereas the bottom band represents endogenous RelB protein.

(c) NF-κB RelB (top) and RelA (bottom) DNA binding activities induced by LPS were monitored with nuclear extracts collected from control or *Traf3*$^{-/-}$ MEFs transduced with empty vector (EV) or a RelB transgene (RelB-TG).

(d) Quantitation of RelB-p50 and RelB-p52 activities in LPS-stimulated *Traf3*$^{-/-}$(RelB-Tg) MEFs; signals were graphed relative to respective RelB-containing dimers basal activity.

(e) Single cell data at indicated time points[7] of the nuclear localization of a retrovirally expressed RelB-GFP fusion protein in response to TNF stimulation of control or *Traf3*$^{-/-}$ MEFs.

(f) Schematic depicting the regulation of RelB by non-canonical or canonical stimuli. RelB may either dimerize with p52 in response to stimulus-induced non-canonical stimuli, or dimerize with p50 and become responsive to canonical stimuli. Cell-type-specific steady-state control of RelB expression and non-canonical pathway activity determines which stimuli activate RelB: at low steady-state levels, RelB is responsive to non-canonical stimuli as reported in MEFs; at high steady-state levels RelB will dimerize not only p52 but also p50, and becomes responsive to canonical stimuli *via* IκBα and IκBε control.

Data shown here are representative of two independent experiments (error bars: s.d.).

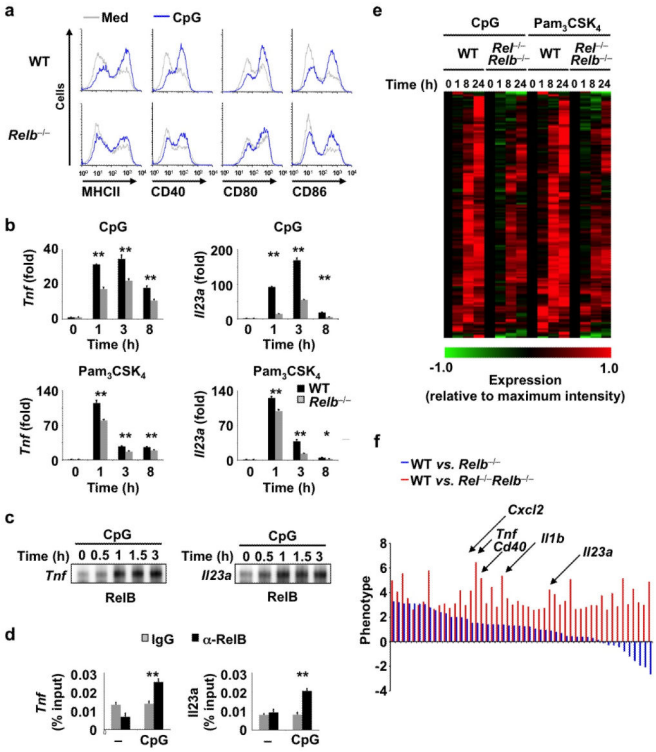

Figure 5. RelB regulates DC activation markers and inflammatory mediators

(a) Analysis of cell surface maker expression in WT and *Relb*$^{-/-}$ BMDCs in response to CpG. Cells untreated (grey) or treated with CpG (blue) or Pam_3CSK_4 (red) for 24 hours were subjected to FACS analysis.

(b) Gene expression analyses of WT and *Relb*$^{-/-}$ BMDCs stimulated with CpG or Pam_3CSK_4 for the indicated time course by qRT-PCR. Signals were graphed relative to respective resting cells.

(c) EMSA with nuclear extracts harvested from CpG-stimulated WT BMDCs using DNA probes containing the κB-site containing promoter sequence from *Tnf* or *Il23a* gene.

(d) Chromatin immunoprecipitation analyses with RelB or IgG control antibodies using cell extracts from WT BMDCs collected prior or 75 minutes after stimulation with CpG. Quantitation of DNA precipitated was performed by qPCR with primers corresponding to the promoter region of indicated genes and graphed relative to input signals.

(e) Microarray mRNA expression analysis from WT and *Rel*$^{-/-}$*Relb*$^{-/-}$ BMDCs stimulated with CpG and Pam_3CSK_4 for indicated time points. Heatmap showing the expression pattern from one experiment in a (log_2) fold induction scale of 157 significant down-regulated genes in *Rel*$^{-/-}$*Relb*$^{-/-}$ BMDCs identified by Significant Analysis of Microarray (SAM). Color scale “1.0” denotes normalized highest expression value of the given gene across time courses.

(f) RelB and c-Rel regulate overlapping sets of genes. The expression phenotype caused by RelB-deficiency was determined for the 50 genes with the most severe expression defect in *Rel*$^{-/-}$*Relb*$^{-/-}$ BMDCs. The list of genes was sorted expression difference between WT and *Relb*$^{-/-}$ BMDCs.

Data shown in (a) (b) (c) (d) are representative of at least three independent experiments (error bars: s.e.m.). *P<0.05, **P<0.01.

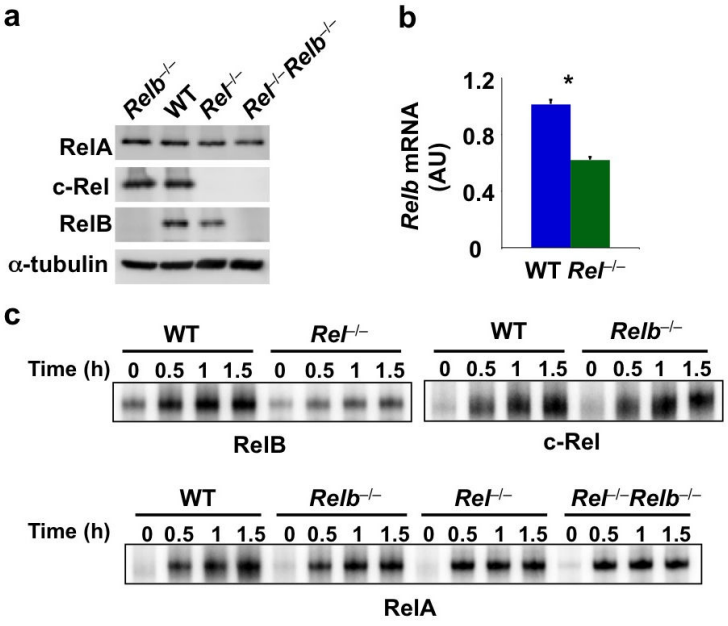

Figure 6. RelB may mediate cRel functions in DCs

(a) Immunoblot for RelA, RelB and cRel of whole cell extracts prepared from indicated gene-deficient BMDCs. α-tubulin serves as loading control.

(b) Amount of *Relb* transcripts was compared by qRT-PCR with mRNA collected from wild type and *Rel*$^{-/-}$ BMDCs and graphed relative to WT cells.

(c) NF-κB DNA binding activities of RelB, c-Rel and RelA induced by LPS in indicated gene-deficient BMDCs were monitored by EMSA.

Data shown are representative of three independent experiments (error bars: s.e.m.).

*P<0.01.